Frequent genetic exchange shapes the pan-mitogenome of the fungal plant pathogen *Fusarium oxysporum*

Anouk C. van Westerhoven[1,2], Jelmer Dijkstra[2], Jose L. Aznar Palop[1], Kyran Wissink[1], Jasper Bell[1], Gert H. J. Kema[2], Michael F. Seidl[1,*]

1. Theoretical Biology & Bioinformatics, Utrecht University, Padualaan 8, 3584 CH, Utrecht
2. Laboratory of Phytopathology, Wageningen University and Research, Droevendaalsesteeg 1, 6708 PB, Wageningen

*Corresponding Author: Michael F Seidl, Theoretical Biology & Bioinformatics, Utrecht University, Padualaan 8, 3584 CH, Utrecht, m.f.seidl@uu.nl

Abstract

Mitochondria are present in almost all eukaryotic lineages. The mitochondrial genomes (mitogenomes) evolve separately from nuclear genomes, and they can therefore provide relevant insights into the evolution of their host species. *Fusarium oxysporum* is a major fungal plant pathogen that is assumed to reproduce clonally. However, horizontal chromosome transfer between strains can occur through heterokaryon formation, and recently signs of sexual recombination have been observed. Similarly, signs of recombination in *F. oxysporum* mitogenomes challenged the prevailing assumption of clonal reproduction in this species. Here, we construct, to our knowledge, the first fungal pan-mitogenome graph of nearly 500 *F. oxysporum* mitogenome assemblies to uncover the variation and evolution. In general, the gene order of fungal mitogenomes is not well conserved, yet the mitogenome of *F. oxysporum* and related species are highly co-linear. We observed two strikingly contrasting regions in the *Fusarium oxysporum* pan-mitogenome, comprising a highly conserved core mitogenome and a long variable region (6-16 kb in size), of which we identified three distinct types. The pan-mitogenome graph reveals that only five intron insertions occurred in the core mitogenome and that the long variable regions drive the difference between mitogenomes. Moreover, we observed that their evolution is neither concurrent with the core mitogenome nor with the nuclear genome. Our large-scale analysis of long variable regions uncovers frequent recombination between mitogenomes, even between strains that belong to different taxonomic clades. This challenges the common assumption of incompatibility between genetically diverse *F. oxysporum* strains and provides new insights into the evolution of this fungal species.

Introduction

Mitochondria are the energy producing organelles of eukaryotic cells (Spinelli and Haigis 2018). Part of their genetic information is encoded apart from the nuclear DNA in a separate mitochondrial genome. This mitochondrial genome evolves at a different rate than the nuclear genome and behaves differently during cell division and reproduction (Barr et al. 2005; Burger et al. 2003; Smith and Keeling 2015). This results in different evolutionary dynamics that make the mitochondrial genome a useful phylogenetic marker which can help to elucidate evolutionary histories separate from the nuclear genome (Christinaki et al. 2022; Ingman et al. 2000).

Although the functions of mitogenomes in eukaryotes are largely conserved, their evolutionary dynamics vary between different eukaryotic lineages, with different mechanisms of inheritance, recombination rates, and mutation rates (Smith and Keeling 2015). In most species, mitochondria are uniparentally inherited, but the mechanisms resulting in uniparental inheritance vary between species and cases of biparental inheritance are also observed (Barr et al. 2005). In most bilateria, the mitochondrial structure is highly conserved and shows little signs of recombination (Ballard and Rand 2005; Ingman et al. 2000). In plants and fungi on the other hand, mitogenomes undergo extensive structural variation and show signs of recombination, horizontal transfer, and intron presence-absence variation (Fritsch et al. 2014; Megarioti and Kouvelis 2020; Smith and Keeling 2015). In fungal mitogenomes, recombination results in highly variable gene order, even within major fungal lineages (Aguileta et al. 2014). In addition to recombination, intron movement drives the structural evolution of fungal mitochondria. Mitochondrial introns are self-splicing mobile elements that can spread throughout and between genomes (Lang et al. 2007; Megarioti and Kouvelis 2020). In many fungal genomes, the expansion of introns is found to cause mitogenome size variations, and introns are often reported to be horizontally transferred (Repar and Warnecke 2017; Wu et al. 2015). These dynamics can provide useful evolutionary insights, for example intron activity can serve as a phylogenetic marker (Wang et al. 2021) and the recombination between mitochondria has revealed signs of introgression in *Saccharomyces* (Christinaki et al. 2022; Leducq et al. 2017; Wu et al. 2015). To further uncover the surprisingly different mechanisms of mitogenome evolution, in depth mitogenome analysis is needed for various species.

Research on mitochondrial evolution has mainly relied on comparing mitochondrial sequences to a reference genome (De Chiara et al. 2020) and as a result highly variable regions in mitochondrial genomes are difficult to analyse. Steps have been taken towards reference free mitogenome analysis using a pan-genomics approach (Brankovics et al. 2018; Wang et al. 2022a), however, large-scale pan-mitogenome analysis have, to our knowledge, not yet been conducted. Recent advances in pangenome variation graphs now allow for reference-free analysis of a large sets of genomes (Eizenga et al. 2020; Sherman and Salzberg 2020), providing a more complete view of gene presence / absence and structural variants (Hickey et al. 2020; Wang et al. 2022b). A pangenome variation graph stores sequences in many different nodes and each genome is represented as a path through connected nodes in the graph. Such a pan-mitogenome provides an excellent tool to analyse mitogenome evolution and enables the reconstruction of structural variants, intron homing, and possibly unique sequences obtained through horizontal transfer events.

The *Fusarium oxysporum* species complex contains several plant pathogens that infect many economically important croups (Edel-Hermann and Lecomte 2019). *F. oxysporum* is well known to exchange accessory chromosomes (Henry et al. 2021; Li et al. 2020; van Westerhoven et al. 2024) and importantly the horizontal transfer of specific accessory chromosomes can transfer pathogenicity between strains (Ma et al. 2010). Between which species this transfer can occur and how often this transfer occurs in nature remains unknown. *F. oxysporum* is considered an asexual fungus, however traces of meiotic recombination in a *F. oxysporum* population have recently been observed, indicating that *F. oxysporum* might in fact undergo sexual recombination (Fayyaz et al. 2023; McTaggart et al. 2021), which would be highly relevant to understand the evolution of this fungal species. The mitochondrial genome of *F. oxysporum* carries a conserved region encoding 14 core mitochondrial genes and a long variable region (LVR) (Al-Reedy et al. 2012; Brankovics et al. 2017). Interestingly, the phylogeny of the mitogenomes is incongruent with the nuclear phylogeny, and thus mitogenomes seem to undergo recombination (Brankovics et al. 2017). This mitochondrial recombination supports the presence of a (para-)sexual cycle that involves the fusion of cells and at least the exchange of mitochondria. To further elucidate the evolutionary history of *F. oxysporum*, we here aim to analyse a large panel of mitogenomes and shed light on the mitochondrial recombination between strains. To this end, we constructed a pangenome variation graphs of nearly 500 *F. oxysporum* mitogenomes to demonstrate frequent and ongoing genetic exchange between distantly related mitochondria, even between strains that belong to

102 distinct taxonomic clades within the *F. oxysporum* species complex. These findings have direct
103 implications for our understanding of the exchange and spread of genetic material, such as
104 pathogenicity chromosomes, between strains of this economically and ecologically important
105 group of fungi.

Results

Fusarium oxysporum mitogenomes have a highly conserved gene order

To understand the diversity of fungal mitogenomes, we first compared the mitogenomes of 706 taxonomically diverse fungal isolates (Fonseca et al., 2021, Table S1), including five *F. oxysporum* mitogenomes. As expected, the gene order is highly variable, also between mitogenomes of closely related fungi (Fig. 1a), which corroborates previous findings (Aguileta et al. 2014) and shows that gene synteny is not well conserved among fungal mitogenomes. Unanticipatedly, mitochondrial gene order is conserved within the class of Sordariomycetes, to which also *F. oxysporum* belongs (Fig. 1a). Next to gene order variation, we also observed a large variation in mitogenome sizes ranging from only 12 kb in *Rozella allomycis* to up to 272 kb in *Ophiocordyceps camponoti-floridani* (Fig. 1b). Importantly, mitogenome size strongly correlates with intron abundance (Fig. 1c, Pearson $r = 0.76$, $p < 0.05$), indicating that recombination and intron expansions drive the variation of fungal mitogenomes.

To study the diversity and evolution of mitochondrial genomes in *F. oxysporum*, we obtained short-read sequencing data of 883 isolates (Table S2). We subsequently removed all isolates that do not belong to the *F. oxysporum* species complex and those where nuclear genome assemblies yielded low BUSCO completeness (Table S2). The remaining 618 *F. oxysporum* isolates are derived from 63 different projects (Table S2) and span the three previously described *F. oxysporum* taxonomic clades (O'Donnell et al. 1998), 61 genomes from clade 1, 402 from clade 2, and 94 from clade 3 (Fig. 1c), and thus represent a wide variety of *F. oxysporum* lineages.

We assembled the mitochondrial DNA using grabB (Brankovics et al. 2016), which resulted in complete and continuous circular mitogenome assemblies for 472 isolates (Fig. 2a, Table S3). The mitochondrial genome assemblies range between 37 and 55 kb in size (Fig. 2b, average 46 kb, Table S3) and have an average GC-content of 31.79%, which is in line with previous assemblies (Al-Reedy et al. 2012; Brankovics et al. 2017). For example, the mitochondrial genome of strain II5 is 49 kb and encodes the 14 *F. oxysporum* core genes, one small subunit RNA gene, and seven additional open reading frames (ORFs) (Fig. 1d). Four of the ORFs are part of an intronic homing endonuclease domain (Megarioti and Kouvelis 2020), but the role of the other three ORFs (ORF151, ORF475, and ORF2229) is currently unknown. In total, between four and 18 additional ORFs were identified per assembled genome and the

139 ORFs can be clustered in to 78 homologous groups, indicating that the pan-mitogenome
140 contains 78 ORFs of unknown function.
141

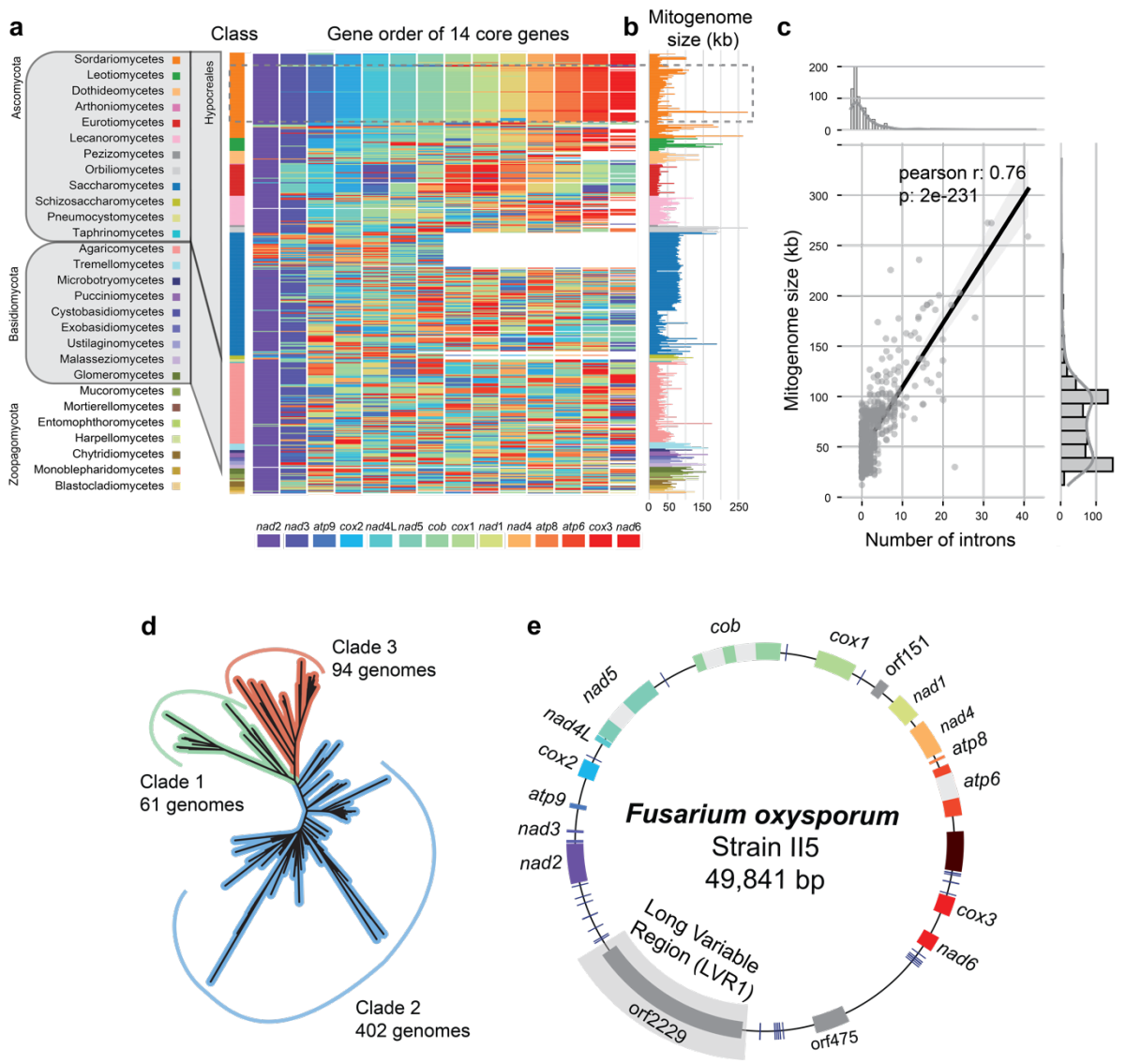

Figure 1 - Mitochondrial genome sizes and synteny are highly variable across fungi. (a) Gene order of 706 fungal mitochondria is highly variable, even between genetically closely related isolates. In contrast, mitochondria from fungi belonging to the Sordariomycetes are remarkably similar. *Fusarium oxysporum* belongs to the Hypocreales within the class of

Sordariomycetes and have a highly conserved mitochondrial gene order. The 14 core genes of *Fusarium* mitochondria (Al-Reedy et al. 2012) are used to visualize the gene order. The mitochondrial genomes are ordered based on the fungal species phylogeny, and the coloured box indicates the identity of the gene and the respective position within the mitogenome; white boxes indicate missing genes. **(b)** Mitochondrial genomes are highly variable in size, even between closely related species **(c)** Mitochondrial genome size variation is largely driven by the number of introns. **(d)** Phylogenetic relationship of the publicly available *F. oxysporum* isolates used in this study. The phylogenetic tree was estimated based on 520 conserved BUSCO genes using FastTree. **(e)** The mitochondrial genome assembly of *F. oxysporum* strain II5 (also known as *F. odoratissimum* strain II5 (Maryani et al. 2019; van Westerhoven et al. 2024) is shown as an example for mitogenomes in the *F. oxysporum* species complex. This mitogenomes contains all 14 core genes (coloured boxes), four introns (grey boxes) and a long variable region (LVR1).

Pan-mitogenome graph reveals highly conserved mitogenome sequences in *Fusarium oxysporum*

To compare the large collection of complete mitochondrial genomes, we constructed a pangenome variation graph using PGGB (Fig. 2c). The pan-mitogenome graph has a length of 87,336 bp and is divided over 15,919 nodes connected by 22,498 edges. On average, a node is present in 189 mitochondrial genomes, and 1,974 (27,552 bp) are present in all isolates (i.e. core), 12,206 are accessory (46,887 bp), and the remaining 1739 are unique to a single strain (12897 bp). To further quantify the variation between mitogenomes, we deconstructed sequence variants directly from the pangenome graph and identified a total of 4,961 variants (2,661 SNPs, 1,698 small indels (<=10 bp), and 602 larger indels (>10 bp) (Fig. 2b); no inversions or translocations were observed (Fig. 2c, Fig S1a). The pangenome graph shows only a single entangled region (Fig. 2c), in which some genomes traverse nodes more than once (Fig. S1b). This region localized at around 10 kb and contains *cox1*, *nad5*, *nad4*, *atp8*, and *atp6* (Fig. 2c). In this region almost all homing endonuclease motifs (HindII, CbaI, BamHI) are located, which occur in different copy numbers in the mitogenomes, and causes the 'knotting' of the graph. Importantly, the limited number of sequence variants as well as the lack of inversions and any other major structural variants demonstrate that the *F. oxysporum* mitochondrial genomes are largely conserved and syntenic, in line with the highly conserved gene order among Sordariomycetes (Fig. 1a).

***Fusarium oxysporum* mitogenomes have few and conserved introns**

Although the core mitogenome is conserved and syntenic between the 472 *F. oxysporum* mitogenomes, the core mitogenome encodes a variable number of introns, ranging from one intron in *nad5* (present in all 472 genomes) to four introns in *nad5*, *cob*, and *atp6* (present in 44 genomes) (Fig. 2a). Three of these introns are clearly visible as alternative paths in the pangenome graph, two in *cob* and one in *atp6* (Fig. 2c,d); the intron in *nad5* is present in all genomes and thus not visible as a variant. All introns are self-splicing group I introns. Group I introns often encode homing endonuclease genes (HEGs) (Lang et al. 2007; Megarioti and Kouvelis 2020), and most introns (*nad5*, *cob* intron-II, and *atp6*) encode 'LAGLIDADG' domains, only the *cob* intron I encodes a 'GIY' domain. This is expected for fungal mitochondrial introns where most introns encode 'LAGLIDADG' domains (Megarioti and Kouvelis 2020).

Homing endonuclease genes in mitochondrial introns are mobile and can spread within and between genomes (Megarioti and Kouvelis 2020; Sellem and Belcour 1997). Using the location of the introns in the pangenome graph, we sought to identify different independent incursions of these introns into the mitogenomes; several intron incursions suggest high intron activity. The *cob* gene has an intron 392 bp after the start of the gene (intron I) and 488 bp after the start of the gene (intron II). We observed that a genome has either only intron I (19% of the genomes) or both intron I and II (10% of the genomes), yet we never observed intron II separately. The conserved location of these two introns indicates that these are the only intron incursions in *cob*. The graph similarly shows that the introns in *atp6* and *nad5* are always located at the same location within the gene and no variants, corroborating previous analyses on a more limited set of mitogenomes (Brankovics et al. 2017) and highlighting that introns in *F. oxysporum* mitochondrial genome are conserved with no additional intron incursions. Interestingly, this contrasts to the intron expansions described in many other fungal mitogenomes (Fonseca et al. 2021; Wang et al. 2021), including those of *Fusarium graminearum* (Brankovics et al. 2018).

In many fungal mitogenomes, the abundance of introns correlates with the total mitogenome size (Fonseca et al., 2021; Wang et al., 2021, Fig. 1c). We similarly observed genome size variation in the 472 mitogenomes (Fig. 2b), yet due to the low number of introns in *F. oxysporum* mitogenomes, the introns at maximum describe up to ~3,000 bp size variation. Consequently, we observed that the total genome size does not strongly correlate with the total number of introns (Pearson r. = 0.39, $p < 0.05$, Fig. S2), highlighting that different regions of the mitogenome must contribute the observed size variation.

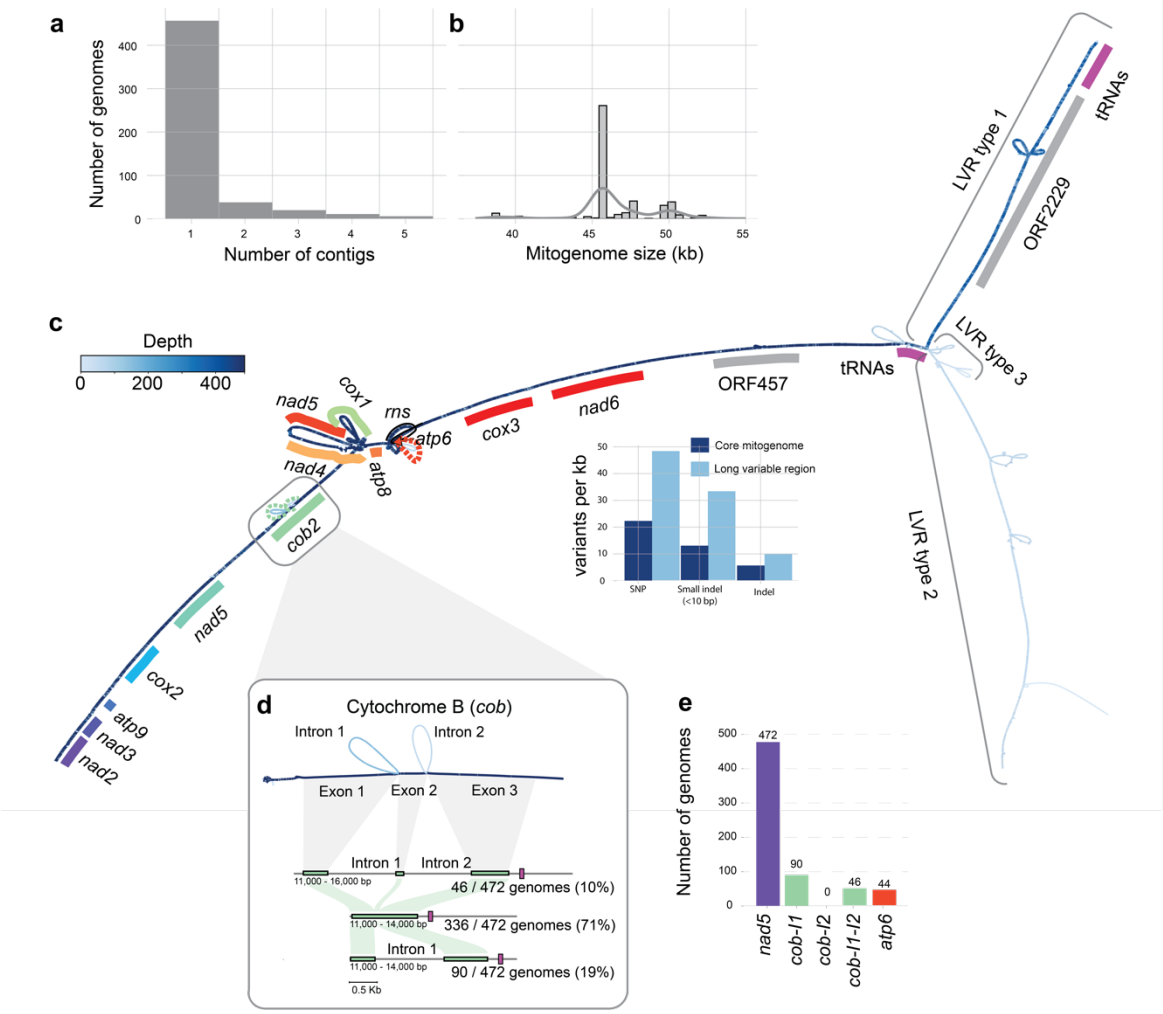

Figure 2 – Pan-mitogenome graph of *Fusarium oxysporum*. (a) The vast majority (472) of *F. oxysporum* mitogenomes were assembled into a single, circular contig. **(b)** The mitogenomes of *F. oxysporum* range in size between 38 – 55 kb. **(c)** The pan-mitogenome graph of *F. oxysporum* shows a highly conserved core region. In addition, the pan-mitogenome reveals three different long variable regions (LVRs) that are present in a subset of the mitogenomes. The dark blue colour indicates this region of the pangenome graph is present in all 472 mitogenome assemblies, while the lighter colours indicate that specific regions are present in fewer mitogenomes. **(d)** Pan-mitogenome graph uncovers variation in three out of four introns (seen as bubbles in the graph). The Cytochrome B (*cob*) gene has two different introns (*cob* I1 and I2), and 136 genomes contain at least one intron in *cob*. However, the pan-mitogenome graph shows there is no variation in the insertion site of the introns. **(e)** In total, four introns are found in the mitogenomes. All mitogenomes contain the intron in *nad5*, and thus this intron is not visible as an alternative path in the pangenome graph.

232 **Variation between mitogenomes is caused by three different long variable regions**
233 Next to the conserved core region, the pan-mitogenome graph also clearly shows the presence
234 of three different long variable regions (LVRs) (Fig. 2c); the LVRs are visible in the pangenome
235 graph, where the graph splits into three different paths. Since shorter variants of the LVR, the
236 absence of an entire LVR, or the presence of chimeric LVRs, might not be visible from the
237 graph directly, we clustered the genomes based on the presence/absence pattern of the nodes in
238 the pan-mitogenome graph (Fig. 3a). The clustering of the LVR reveals the presence of only
239 three distinct LVRs types, in line with the observations from the pangenome graph (Fig. 2c).
240 Consequently, no genome lacks the LVR or contains significantly shorter or chimeric variants.
241 However, we do observe some variation in the LVRs, visible as the bubbles in the pangenome
242 graph (Fig. 2c). Interestingly, previous reports based only on a small subset of *F. oxysporum*
243 mitogenome report the same three long variable regions (Brankovics et al. 2017), and thus,
244 unanticipatedly, the inclusion of hundreds of diverse mitogenomes does not reveal additional
245 LVRs.
246
247 To further analyse the various types of mitogenomes in *F. oxysporum*, we also clustered
248 the complete pangenome graph. This clustering revealed the same three clusters of
249 mitochondrial genomes (Fig. 3a). Importantly, separation into these three mitochondrial types
250 is caused by the LVR, as the same three clusters are obtained by clustering solely the presence-
251 absence of the LVR (adjusted rand index = 0.98, Fig. 3c). In contrast to the similarity between
252 the complete graph and the LVRs, clustering based on the core mitogenome region uncovered
253 four vastly different clusters (ARI = -0.02), suggesting that the observed variation between
254 mitochondrial genomes is largely driven by LVRs and that the LVR evolves separately from
255 the core mitogenome.
256
257 **Long variable regions are unique to the *Fusarium* genus**
258 Only three distinct LVRs occur in *F. oxysporum* (Fig 3a; Brankovics et al. 2017), yet no
259 biological function could be assigned nor has the origin of these regions been elucidated. The
260 three LVRs are localized between two tRNA clusters and encode different open reading frames
261 (ORFs) (Fig. 2c). The LVRs vary largely in size; LVR1 is approximately 10 kb, LVR2 18 kb,
262 and LVR3 is the smallest with approximately 5 kb. The LVR size is strongly correlated with
263 the size of the complete mitogenome (Pearson $r = 0.89$, $p < 0.05$, Fig. S2), demonstrating that
264 genome-size variation between *F. oxysporum* mitogenomes is driven by the type of LVR.
265

The different LVRs have an unequal distribution between *F. oxysporum* strains (Fig. 2c). LVR1 is the most abundant and is detected in 83% of the mitogenomes, while LVR2 is found in only 6%, and LVR3 in 11% of the genomes. Importantly, the LVRs share no similarity to each other (Fig. S3), and the lack of homology as well as the absence of degenerated or chimeric LVRs suggests that the different LVR types are not derived from each other. It currently remains unknown why only these three LVRs are observed. Moreover, the function of the LVRs so far remains unelucidated, as we did not predict any known protein domains in the ORFs.

To uncover the origin of the different LVRs, we sought to detect homologous regions in 706 diverse fungal mitogenomes (Fonseca et al. 2021) (Table S1). We observed that LVR1 is present in different *Fusarium* species, whereas LVR2 and LVR3 is only found in *F. oxysporum* (Fig. S4); outside the *Fusarium* genus, only small hits can be detected (Fig. S4). We also queried the non-redundant nucleotide database, excluding *Fusarium* species, and similarly only observed small (< 200 nt) matches (Table S6-8), suggesting that the most likely origin of these regions is within the *Fusarium* genus.

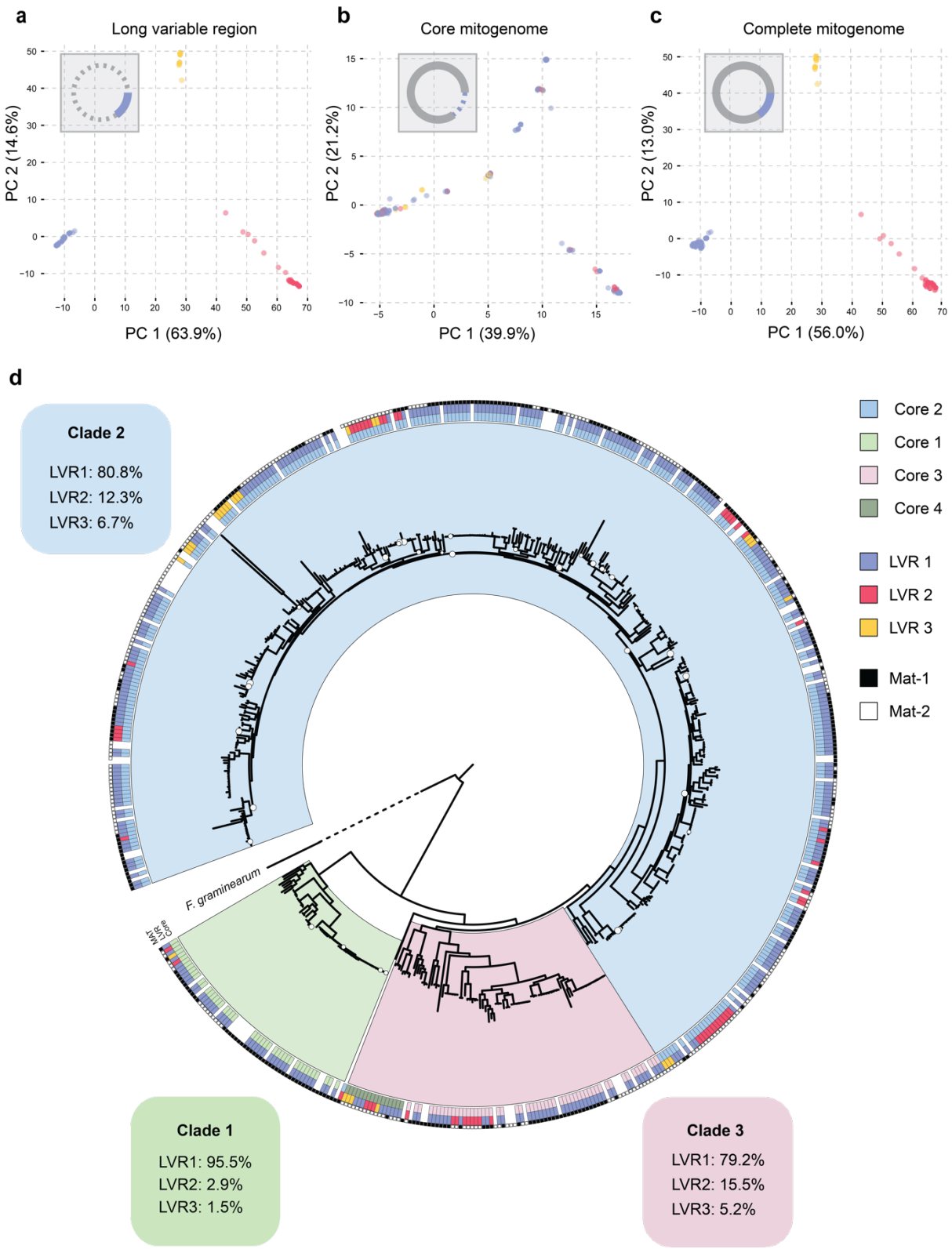

Figure 3 – Long variable regions are different from the core-mitogenome and do not correspond to lineages in the nuclear phylogeny. Principal component analysis (PCA) based on the presence / absence patterns of the nodes in **(a)** LVRs, **(b)** the core mitogenome, and **(c)** the complete pan-mitogenome graph. The core mitogenome results in four different clusters, the four groups are different from the groups obtained based on the complete pangenome graph (adjusted rand index = -0.02) and from the groups based on the long variable region (adjusted rand index = -0.02). **(d)** The nuclear phylogeny of 472 *F. oxysporum* assemblies is based on

291 4213 single-copy BUSCO genes and maximum-likelihood analysis (2,495,112 aa positions).
292 The three well-recognized clades in *F. oxysporum* (O'Donnell et al. 1998) are clearly visible
293 based on the nuclear phylogeny. The first outer ring indicates where the isolate clusters based
294 on the core mitogenome. These core-mitogenome clusters as defined by the PCA (panel **b**) are
295 similar to the taxonomic clades visible from the nuclear phylogeny. For one group of isolates
296 in clade 3 the core mitogenomes cluster in the middle of the PCA (group core 4).The outer ring
297 indicates the assigned clusters based on the presence of different LVRs (panel **a**), and these do
298 not follow the nuclear phylogeny as all LVR types can be identified in all three *F. oxysporum*
299 clades.
300

301 **LVR types are incongruent with the nuclear phylogeny**

302 To trace the evolution LVRs in *F. oxysporum*, we compared the occurrence of LVRs and core-
303 regions of the mitogenomes to a nuclear phylogeny that is based on nuclear-encoded,
304 conserved, single-copy orthologs (Fig. 3d). Importantly, the core mitogenomes follow the
305 nuclear phylogeny (Fig. 3d), and each core mitogenome can be assigned to a single
306 phylogenetic clade. In contrast, the three different LVRs do not follow the nuclear phylogeny,
307 and all three LVR-types occur in all three taxonomic clades (Fig. 3d). Interestingly, even
308 genetically related *F. oxysporum* isolates can carry a different LVR. For example, two isolates
309 in clade 2 have a highly similar core mitogenome (>99.9% identity, eleven SNPs, 14 small
310 indels <= 10 bp, and four indels), yet they have different LVRs (LVR1 and LVR2) with only
311 limited similarity around the tRNAs sequences (Fig 4b). Out of 44 groups of closely related
312 genomes (branch length < 0.000001; on average five genomes per group), four groups have
313 more than one LVR, indicating that these highly similar genomes encode different LVRs.
314

315 The incongruence between LVRs and the nuclear phylogeny might be due to horizontal
316 transfer. In plants and fungi, horizontal transfer between mitochondria has been reported as
317 well as the exchange of entire mitogenomes (Bergthorsson et al. 2004; Wu et al. 2015). The
318 exchange between mitogenomes could result in heteroplasmy, i.e. the presence of two or more
319 distinct mitochondrial populations within a single individual. To detect the occurrence of
320 heteroplasmy, we compared the sequencing data of each of 472 isolates directly to the
321 pangenome graph. We expected bi-allelic variants to indicate heteroplasmy, yet we did not
322 observe any diploid variants in any of the isolates, neither in the core nor in the LVRs,
323 indicating that heteroplasmy, if existent, is a very transient state in *F. oxysporum*. We then
324 sought to experimentally examine if LVRs could be horizontally transferred between *F.*
325 *oxysporum* stains by inducing a swap of LVRs between two related strains (strain NRRL36117
326 (LVR1), C135 (LVR2)). Although heterokaryons were successfully formed (Fig. S5), no
327 exchange of mitochondria could be observed. Out of 47 spores derived from heterokaryotic

328 mycelia, the nuclear genome and LVR of 44 spores was similar to NRRL36117 and only three
329 spores were positive for C135 (Fig. S5). One of the spores remained a heterokaryon and was
330 positive for both NRRL36117 and C135 primers. This means we observed an unequal
331 distribution of the two strains after heterokaryon formation, since most of the spores resemble
332 NRRL36117. This is in line with previous reports that suggest that only one genome is
333 maintained after heterokaryon formation (Shahi et al. 2016).
334
335 **Long variable regions are frequently exchanged**
336 Possibly, the LVRs of mitochondria could be transferred between strains, yet the three different
337 types can also be present in the ancestor. We expect that if all three LVRs are ancestral, their
338 evolution would be in line with the nuclear genomes. We therefore constructed phylogenetic
339 trees for the three LVRs and observed for LVR2 and LVR3 that genetically distant isolates can
340 share the same or very similar LVR. For example, LVR3 from Fo6 (clade 1), Fo13 (clade 4),
341 and Fo5 (clade 2) (all endophytes sampled from tomato plants in Australia) is highly similar
342 (99.1 % identity, four small indels <= 10 bp), whereas the three genomes all belong to different
343 taxonomic clades, and the core mitogenomes has 184 variants (84 SNPs, 73 small indels <
344 10bp, and 27 indels > 10 bp) as well as variation in intron presence / absence (Fig. 4c,d). We
345 added an additional isolate from clade 2 carrying LVR3. This shows that the core mitogenomes
346 are highly similar between the clade 2 isolates, yet LVR3 is only 96.1 % similar. Thus, LVRs
347 from genetically distinct isolates, even belonging to a different phylogenetic clade, can be
348 similar, while the core mitogenome shows variation between the strains. The unexpected
349 similarity of LVRs between genetically distant strains can possibly be explained by the transfer
350 of the LVR between isolates.
351
352 To further analyse the exchange of LVRs between different *F. oxysporum* clades, we
353 directly compared the phylogenetic tree based on the LVRs to the phylogenetic tree based on
354 the nuclear genome and quantified the phylogenetic distances (estimated by the branch length)
355 between LVRs of isolates belonging to the same phylogenetic clade and between LVRs of
356 isolates belonging to different clades. Interestingly, the phylogeny of LVR1 shows three distinct
357 clusters similar to the three clades found in the nuclear phylogeny (Fig. S6). Thus, isolates with
358 LVR1 belonging to the same clade typically carry a similar LVR, separated by a low
359 phylogenetic difference (median branch length = 0.004), whereas isolates belonging to
360 different clades have more dissimilar LVR1s (median branch length = 0.029, p = 0.00, Fig. 4f).
361 This suggests that LVR1 evolves in line with the nuclear genome and that LVR1 was likely

present in the last common ancestor of *F. oxysporum*. However, the pattern for LVR2 and LVR3 is remarkably different. Here, the similarity of LVRs between isolates belonging to the same taxonomic clade (LVR2: mean branch length = 0.0132, LVR3: mean branch length = 0.006) is close to the similarity between LVRs of isolates belonging to different taxonomic clades (LVR2: mean branch length = 0.027, LVR3: mean branch length = 0.0136), which is in line with the highly similar LVR3 that can be found in three isolates from different taxonomic clades (Fig. 4c-e, Fig. S8). These results not only suggest that LVRs can be exchanged between strains, but that this exchange can occur between genetically distant strains that belong to different taxonomic clades.

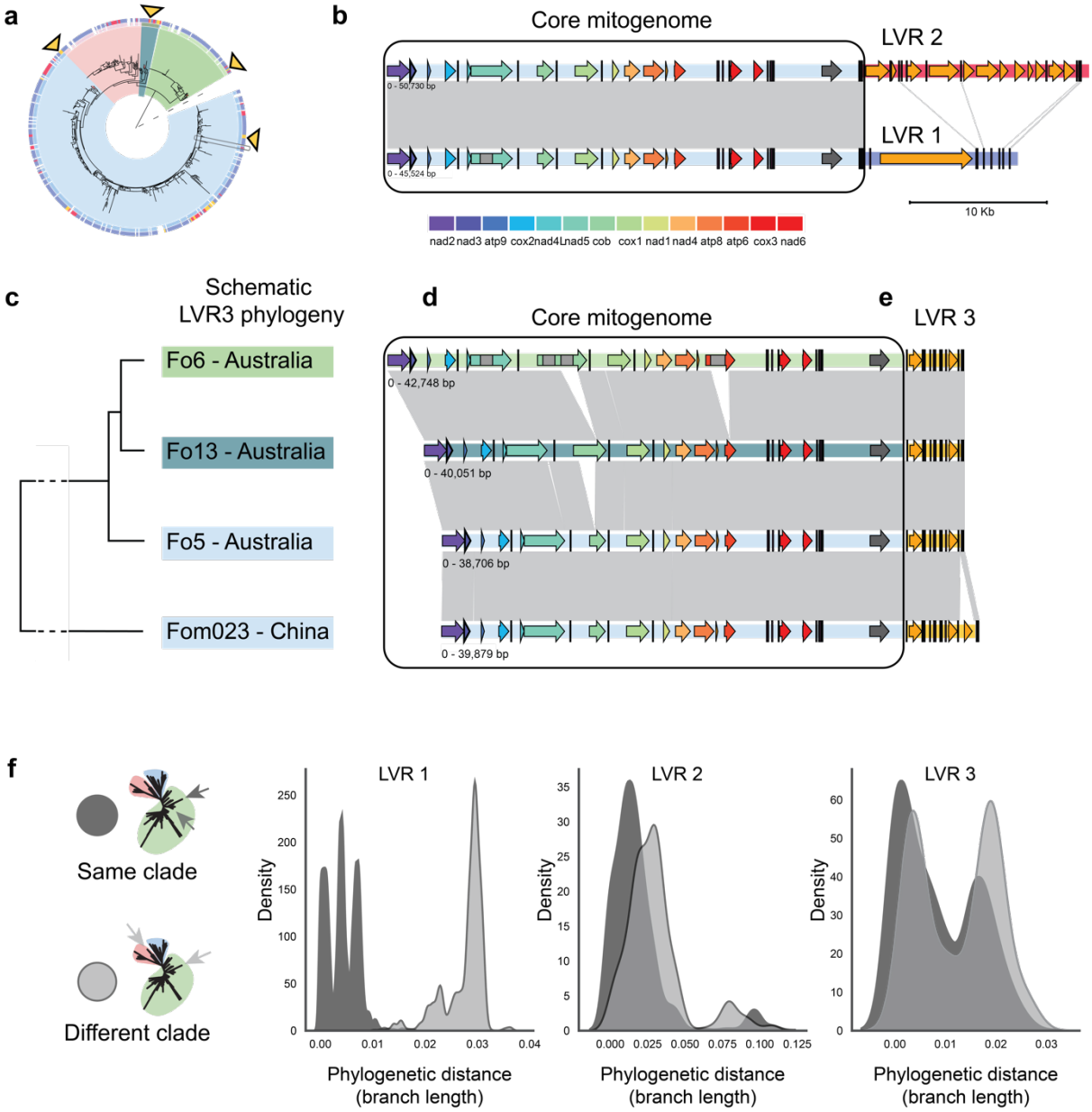

Figure 4 – LVRs are frequently exchanged between *F. oxysporum* isolates of different taxonomic clades. **(a)** Simplified nuclear phylogeny of *F. oxysporum* strains (see Fig. 3 for details), grey box indicates the strains compared in panel **b** and arrows indicate the strains compared in panel **c**. **(b)** Comparison of two closely related strains with different LVRs. Light blue region is the core mitogenome found in clade 2. The core mitogenome is highly similar, whereas LVR1 and LVR2 do not show any similarity, apart from similar tRNA genes. **(c)** Schematic tree of LVR from four different strains belonging to different clades in the nuclear phylogeny (Fo6 clade 1, Fo13 clade 4, and Fo5 clade 2). **(d)** Comparison of the core mitogenome of three strains from a different clade carrying the same LVR3 variant, as well as a clade 2 strain carrying a different LVR3 variant (Fom023). The core mitogenome shows variation in intron content as well as some small intergenic variants. However, the LVR is highly similar (99.1%) between the isolates **(e)**. Fom023 encodes an extra open reading frame in the LVR3. **(f)** Branch length between all possible pairs in each LVR phylogeny. For LVR1 the median branch length is higher between strains belonging to different clades (0.029) than for strains belonging to the same clade (0.004). For LVR 2 and LVR3, the median branch length between strains belonging to different clades (LVR2 = 0.027, LVR3 = 0.0136) is closer to the median branch length between strains belonging to the same clade (LVR2 = 0.0132, LVR3 = 0.006) and the distribution of branch lengths looks similar. This means that a LVR from isolates from different clades can be highly similar.

392 **Discussion**

393 The evolutionary history of mitogenomes can provide direct insights into the evolutionary
394 history of their host species (Christinaki et al. 2022; Ingman et al. 2000). Pangenome graphs
395 recently emerged as a novel framework to facilitate analyses of large genomic datasets and are
396 a useful tool to uncover novel biological insights (Li et al. 2022; Wang et al. 2022b). We here
397 constructed, to our knowledge, the first pan-mitogenome of a filamentous fungus, based on
398 hundreds of genetically diverse *F. oxysporum* isolates. Many members of the large and diverse
399 *F. oxysporum* species complex are major plant pathogens, and for a long time these have been
400 considered to only reproduce clonally. However, recently signatures of sexual recombination
401 have been observed, indicating the presence of a sexual cycle in this presumed asexual fungus
402 (Fayyaz et al. 2023; McTaggart et al. 2021). Previously analyses of the mitogenome of *F.*
403 *oxysporum* provided initial evidence for mitochondrial recombination (Brankovics et al. 2017),
404 and we here sought to further elucidate these mitochondrial dynamics and the patterns of
405 recombination. Our pan-mitogenome graph uncovers highly conserved and syntenic core
406 mitogenomes. In contrast, we could clearly distinguish three distinct types of long variable
407 regions (LVRs), which explain most of the mitochondrial variation in *F. oxysporum*. Whereas
408 the core mitogenome evolves in line with the nuclear genome, the LVRs are incongruent with
409 the nuclear phylogeny. Importantly, we found highly similar LVRs between genetically distant
410 isolates, even between isolates from a different phylogenetic clade, which shows that genetic
411 exchange can occur between distantly related *F. oxysporum* isolates, suggesting that distant
412 taxonomic clades, contrary to previous expectations, are not isolated. This seemingly
413 unrestricted capacity to recombine has significant implications in the evolution of *Fusarium*,
414 for instance in their ability to horizontally exchange accessory chromosomes.

415

416 LVRs have been discovered previously in *Fusarium* and are found to encode open
417 reading frames (ORFs) of unknown function (Al-Reedy et al. 2012; Brankovics et al. 2017).
418 Similarly, ORFs of unknown function are described, for example in other fungal species (Jelen
419 et al. 2016) and bivalves (Milani et al. 2013). In the latter case, the unknown ORFs seems to
420 be derived from viral origin and play a role in the inheritance of mitochondria (Milani et al.
421 2013). However, these described ORFs are shorter than the ORF found in the LVR in the
422 *Fusarium* genus and the origin and function of these ORFs remain unclear. Notably, we here
423 observed only three different types of LVRs in the *F. oxysporum* pan-mitogenome and even
424 though we included nearly 500 diverse isolates, no degenerated or chimeric variants could be
425 observed. Previous studies suggested that LVRs evolve similar to intergenic regions. We

426 similarly determined that LVRs have a higher density of variants per kb than the core
427 mitogenome. The lack of homologous sequences in other species hampers our attempts to
428 further elucidate the origin of the LVR. The abundance of LVR1, together with the presence of
429 LVR1 in other *Fusarium* species members and the similarity to the nuclear phylogeny, suggests
430 that this LVR is most likely ancestral. However, we did not find similarity between LVR1,
431 LVR2, and LVR3, showing that these types do not originate from recombination with LVR1 or
432 through degeneration. Moreover, LVR2 and LVR3 do not follow the nuclear phylogeny, and
433 we hypothesize that the LVRs are exchanged through recombination between two mitochondria
434 encoding a different LVR. Notably, while frequent recombination of LVRs between isolates
435 occurs, we did not detect any signature of recombination in the core genome. The lack of
436 recombination in the core mitogenome is in line with the highly conserved gene order among
437 *F. oxysporum* species and even among the class of Sordariomycetes, as gene order shuffling is
438 the result of recombination (Aguileta et al. 2014). It is conceivable that the tRNA genes that
439 flank the LVRs are particularly prone to recombination and the clustering of these tRNAs at
440 the LVRs and sparsity of tRNAs in the core genome possibly drives the observed pattern of
441 recombination (Fritsch et al. 2014; Pratt-Hyatt et al. 2006). Alternatively, selection against
442 additional recombination sites that affect the core mitogenome can result in a lack of observed
443 recombination.
444
445 *F. oxysporum* strains belonging to different taxonomic clades can carry surprisingly
446 similar LVRs, which suggest that these isolates can recombine regardless of the extensive
447 genetic differentiation between the nuclear genomes. Frequent recombination, resulting in
448 exchange of LVRs, between diverse isolates is significant, as the prevailing thought is that
449 recombination does not occur between taxonomic clades (Brankovics et al. 2017; McTaggart
450 et al. 2021). To interpret the incongruent phylogeny between the mitogenome and the nuclear
451 genome, it is imperative to understand the mode of mitochondrial inheritance. In fungi, both
452 uniparental and biparental mitochondrial inheritance has been described (Barr et al. 2005), and
453 recombination of mitochondria has been observed. In yeast, for example, biparental inheritance
454 results in short-lived heteroplasmy, during which mitochondrial recombination can occur (Wu
455 et al. 2015). Although *F. oxysporum* has for long been considered to lack a sexual cycle, and
456 thus the mitochondria should be inherited clonally, conidial anastomosis in filamentous fungi
457 allow for the fusion of cells of distantly related isolates (Read et al. 2012; Roca et al. 2003). In
458 this process, the cytoplasm of cells is connected, which enables the movement of mitochondria
459 (Kurian et al. 2018; Mehta and Baghela 2021; Roca et al. 2003; Vangalis et al. 2021). Upon

fusion, only one nucleus is maintained in *F. oxysporum* (Kurian et al. 2018), and it has been indicated in four strains that the mitotype of the acceptor is maintained upon horizontal transfer events (van Dam et al. 2017). This is in line with our own observations that suggest that after heterokaryon formation, only one nucleus and one mitogenome is maintained. Our data suggest that, even though we observed patterns of frequent recombination between mitochondria of extant strains, this is likely an infrequent event in nature. Notably, we observed exchange between strains that were sampled from the same geographic location or similar environment, as physical proximity of isolate is a prerequisite of genetic exchange. However, knowledge on mitochondrial fusion, fission, and recombination upon heterokaryon formation remains limited.

In fungi, horizontal gene and chromosome transfer occurs (Habig et al. 2021; Mehrabi et al. 2011). Extensive horizontal chromosome transfer has been observed in *F. oxysporum*, even between distantly related strains that are not vegetatively compatible, which means the strains cannot form a viable heterokaryon (Fokkens et al. 2018; Shahi et al. 2016; Vlaardingerbroek et al. 2016). The horizontal transfer of nuclear DNA over large genetic distances is analogous to the exchange of mitochondrial LVRs over large genetic distances. Yet, the exchange of chromosomes in *F. oxysporum* has only been observed between strains belonging to the same clade (Fokkens et al. 2018; Shahi et al. 2016; Vlaardingerbroek et al. 2016), whereas we observe recombination of mitochondria between strains belonging to different clades. This suggests that exchange of accessory chromosomes over large genetic distances might be possible, and that the clades are not genetically isolated as has been previously thought (Brankovics et al. 2017; McTaggart et al. 2021). It is important to note, however, that it is currently unclear how the dynamics of the mitogenome relate to nuclear genomes and, to our knowledge, the relationship between mitochondrial transfer and horizontal gene transfer has not been studied. Examples of mitochondrial exchange can form an excellent starting point to relate the exchange of mitochondrial material to the exchange between nuclear genomes.

The transfer of mitochondria between cells has been observed in various other species. For example, mitochondria can be exchanged between human tissues (Borcherding and Brestoff 2023) and between plant cells, for instance, upon grafting (Gurdon et al. 2016). Transfer of mitochondria enables mitochondrial recombination between varying mitogenomes. Extensive horizontal transfer of mitochondria has been reported in the basal angiosperm

494 *Amborella*, where the mitochondrial DNA contains material from great phylogenetic distances
495 like mosses green algae but also other angiosperms (Bergthorsson et al. 2004; Rice et al. 2013).
496 However, it is currently unknown what mechanisms enable these mitochondrial transfers over
497 large evolutionary distances.
498
499 Recent developments in mitogenome analyses have uncovered novel insights in
500 mitochondrial biology, and the remarkable evolutionary dynamics of mitogenomes are
501 becoming clear (Burger et al. 2003; Gurdon et al. 2016; Rice et al. 2013). This raises the
502 questions how this genetic variation in mitochondrial genomes is established and how the
503 evolutionary dynamic of mitochondria links to the biology and the evolution of their host
504 species. We here demonstrate, by using *F. oxysporum* mitogenomes as an example, that pan-
505 mitogenomes provide an important framework to elucidate mitochondrial genome evolution
506 not only in fungi but also in other eukaryotes, which can ultimately help to understand their
507 evolution.
508
509

Materials and Methods

Mitogenome assemblies

To determine the gene-order and intron content in fungal mitochondria, we downloaded 706 publicly available fungal mitogenomes (Fonseca et al. 2021). These genomes have been annotated using MFannot followed by manual curation (Fonseca et al. 2021).

To study the evolution of *Fusarium oxysporum* mitogenomes, we downloaded all available 813 short-read dataset from the NCBI short read archive (SRA) on September 11th, 2022 (Table S2). Additionally, we added 70 Fusarium oxysporum strains infecting banana (van Westerhoven et al. 2024). Because all data is obtained from different sources, we checked the dataset to make sure the short-read data is correctly labeled and of sufficient quality. We filtered the dataset on BUSCO completeness (version 5.3.1, hypocreales_odb10), selecting isolates containing more than 90% of the single copy BUSCO genes. Based on 4213 BUSCO genes we estimated the maximum likelihood phylogeny using FastTree version 2.1.11 (Price et al. 2010). We subsequently removed all isolates that were not associated to *Fusarium oxysporum* (details for data acquisition and filtering, SI methods).

Assembly and annotation

We assembled all *Fusarium oxysporum* short reads using GrabB version 1 (Brankovics et al. 2016), providing six complete *Fusarium oxysporum* mitogenomes from the NCBI database (NCBI accessions: MT010933.1, KR952337.1, AY945289.1, MF155191.1, MT269799.1, and MT010933.1) to bait mitochondrial reads from the short-read data. To ensure high-quality and contiguous mitogenome assemblies, we continued only with the assemblies that were successfully assembled into a single contig.

The assembled mitogenomes were subsequently annotated using MFannot version 3.0, specifying the translation frame table 4 and allowing for small motif and homing endonuclease domain annotation (Lang et al. 2023). In addition to known mitochondrial genes, many ORFs were annotated per genome. To identified homologous ORFs in the different annotations, we clustered ORFs with CD-hit version 4.8.1 (Li and Godzik 2006), with sequence identity of 0.8 and an alignment coverage of the shortest sequence of 0.8. Protein domains in these ORFs were identified using Interproscan version 5.67 (Quevillon et al. 2005).

Graph construction

To build the pangenome variation graph, we used pangenome graph builder (PGGB) version 0.3.0 (Garrison et al. 2023). The segment size (-s) was set to 3000 bp and the percent identity was calculated using mash triangle (Ondov et al. 2016), resulting in a percent identity (-p) of 97.523., asm10. The graph was visualized using Bandage version 0.9.0 (Wick et al. 2015). We further analyzed the graph using odgi version 0.8.2 (Guarracino et al. 2022), and general graph statistics were obtained using odgi stats. To annotate the graph, we provided the annotation of the *F. oxysporum* stains TR4 II5 mitogenome to odgi position, the resulting csv file was used to extract loci and to determine the gene locations in the graph. To determine the variants in the graph, we used the deconstruct command from vg-tools version 1.49.0 (Garrison et al. 2018) specifying flag -a to get nested variants, to create a vcf file of the variants in the graph.

To analyze potential heteroplasmy of mitogenomes in *Fusarium oxysporum*, we aligned all unassembled short reads to the graph using vg giraffe version 1.49.0 (Sirén et al. 2021) and obtained variants using vg call (Hickey et al. 2020) with the diploid flag. The number of diploid variants were used to estimate the presence of heteroplasmy.

Analysis of LVRs

To analyze the different types of mitogenomes the graph, we obtained the node presence absence based on odgi matrix. This matrix was used for a principal component analysis using scikit learn version 0.24.2 (Pedregosa et al. 2011).

To construct the phylogeny of the LVRs, we extracted the LVR sequence from all mitogenomes. For each genome, we determined the genomic coordinates belonging to the LVR and extracted the fasta files using bedtools getfasta (Quinlan and Hall 2010). We aligned the LVR sequences using mafft version 7.520 (Katoh et al. 2002) and used these alignment to construct a phylogeny using RAxML version 1.2.0 (Stamatakis 2014) with the model 'GTR+G'. We calculated the pairwise branch length between each pair of isolates in the LVR phylogeny using Biopython version 1.79 (Cock et al. 2009) and grouped the pairs in to two categories; either both genomes belong to the same clade or belonging to a different clade. To plot the similarity between mitogenomes we used Pygenomeviz version 0.4.4 (Shimoyama 2022). The genome alignments were calculated using mummer version 4 (Marçais et al. 2018).

We searched the presence of the three LVRs in the 706 fungal mitogenomes (Supplementary table S1), using one representative of each LVR (LVR1; M1, LVR2; NRRL36117; LVR3; SRR10428567 – Fo6) as a query for BLAST. To find potential hits with isolates not included in the set of fungal mitogenomes, the LVRs were searched against the BLAST database (accessed 15-05-2024), excluding hits with members of the *Fusarium* genus.

We further assayed the behavior of mitochondria upon heterokaryon formation of genetically related strains carrying different LVRs. To test if the mitotypes can be swapped between isolates, we created single-spore isolates from the heterokaryon and tested the LVR type present in this isolate (for details, see SI methods).

Data accesses

All mitogenome assemblies and gene annotations are available on Figshare (10.6084/m9.figshare.26063593). The scripts used in this study are available on Github (https://github.com/Anouk-vw/pan-mitogenome_FOSC).

Competing interest statement

The authors declare no competing interest.

Acknowledgements

ACW, JD, and GHJK were supported by the Bill and Melinda Gates Foundation, grant number AG - 4425. The funders had no role in study design, data collection and analysis, decision to publish, or preparation of the manuscript. We thank Like Fokkens for her feedback on the manuscript.

Author contributions

ACW performed analysis and data analyses, and wrote the draft manuscript, with support of MFS. J.D conducted experiments. L.A.P, K.W and J.B were involved in the data analysis and interpretation. All authors contributed to editing of the manuscript. GHJK and MFS supervised the project.

References

Aguileta G, de Vienne DM, Ross ON, Hood ME, Giraud T, Petit E, Gabaldón T. 2014. High variability of mitochondrial gene order among fungi. *Genome Biol Evol* **6**: 451–465. https://www.ncbi.nlm.nih.gov/pmc/articles/PMC3942027/ (Accessed November 3, 2023).

Al-Reedy RM, Malireddy R, Dillman CB, Kennell JC. 2012. Comparative analysis of Fusarium mitochondrial genomes reveals a highly variable region that encodes an exceptionally large open reading frame. *Fungal Genet Biol* **49**: 2–14.

Ballard JWO, Rand DM. 2005. The population biology of mitochondrial DNA and its phylogenetic implications. *Annual Review of Ecology, Evolution, and Systematics* **36**: 621–642. https://www.annualreviews.org/content/journals/10.1146/annurev.ecolsys.36.091704.175513 (Accessed April 23, 2024).

Barr CM, Neiman M, Taylor DR. 2005. Inheritance and recombination of mitochondrial genomes in plants, fungi and animals. *New Phytologist* **168**: 39–50. https://onlinelibrary.wiley.com/doi/abs/10.1111/j.1469-8137.2005.01492.x (Accessed February 9, 2024).

Bergthorsson U, Richardson AO, Young GJ, Goertzen LR, Palmer JD. 2004. Massive horizontal transfer of mitochondrial genes from diverse land plant donors to the basal angiosperm Amborella. *Proceedings of the National Academy of Sciences* **101**: 17747–17752. https://www.pnas.org/doi/full/10.1073/pnas.0408336102 (Accessed April 11, 2024).

Borcherding N, Brestoff JR. 2023. The power and potential of mitochondria transfer. *Nature* **623**: 283–291. https://www.nature.com/articles/s41586-023-06537-z (Accessed May 17, 2024).

Brankovics B, Kulik T, Sawicki J, Bilska K, Zhang H, Hoog GS de, Lee TA van der, Waalwijk C, Diepeningen AD van. 2018. First steps towards mitochondrial pan-genomics: detailed analysis of *Fusarium graminearum* mitogenomes. *PeerJ* **6**: e5963. https://peerj.com/articles/5963 (Accessed April 20, 2022).

Brankovics B, van Dam P, Rep M, de Hoog GS, J. van der Lee TA, Waalwijk C, van Diepeningen AD. 2017. Mitochondrial genomes reveal recombination in the presumed asexual *Fusarium oxysporum* species complex. *BMC Genomics* **18**: 735. https://doi.org/10.1186/s12864-017-4116-5 (Accessed April 18, 2022).

Brankovics B, Zhang H, Diepeningen AD van, Lee TAJ van der, Waalwijk C, Hoog GS de. 2016. GRAbB: selective assembly of genomic regions, a new niche for genomic research. *PLOS Computational Biology* **12**: e1004753. https://journals.plos.org/ploscompbiol/article?id=10.1371/journal.pcbi.1004753 (Accessed April 20, 2022).

Burger G, Gray MW, Franz Lang B. 2003. Mitochondrial genomes: anything goes. *Trends in Genetics* **19**: 709–716. https://www.sciencedirect.com/science/article/pii/S0168952503003044 (Accessed April 23, 2024).

Christinaki AC, Kanellopoulos SG, Kortsinoglou AM, Andrikopoulos MA, Theelen B, Boekhout T, Kouvelis VN. 2022. Mitogenomics and mitochondrial gene phylogeny decipher the evolution of Saccharomycotina yeasts. *Genome Biology and Evolution* **14**: evac073. https://doi.org/10.1093/gbe/evac073 (Accessed December 20, 2023).

Cock PJA, Antao T, Chang JT, Chapman BA, Cox CJ, Dalke A, Friedberg I, Hamelryck T, Kauff F, Wilczynski B, et al. 2009. Biopython: freely available Python tools for computational molecular biology and bioinformatics. *Bioinformatics* **25**: 1422–1423. https://doi.org/10.1093/bioinformatics/btp163 (Accessed May 8, 2024).

De Chiara M, Friedrich A, Barré B, Breitenbach M, Schacherer J, Liti G. 2020. Discordant evolution of mitochondrial and nuclear yeast genomes at population level. *BMC Biol* **18**: 1–15. https://bmcbiol.biomedcentral.com/articles/10.1186/s12915-020-00786-4 (Accessed April 25, 2024).

Edel-Hermann V, Lecomte C. 2019. Current status of *Fusarium oxysporum formae speciales* and races. *Phytopathology* **109**: 512–530.

Eizenga JM, Novak AM, Sibbesen JA, Heumos S, Ghaffaari A, Hickey G, Chang X, Seaman JD, Rounthwaite R, Ebler J, et al. 2020. Pangenome graphs. *Annual Review of Genomics and Human Genetics* **21**: 139–162. https://www.annualreviews.org/content/journals/10.1146/annurev-genom-120219-080406 (Accessed April 26, 2024).

Fayyaz A, Robinson G, Chang PL, Bekele D, Yimer S, Carrasquilla-Garcia N, Negash K, Surendrarao A, von Wettberg EJB, Kemal S-A, et al. 2023. Hiding in plain sight: genome-wide recombination and a dynamic accessory genome drive diversity in *Fusarium oxysporum* f.sp. *ciceris*. *Proceedings of the National Academy of Sciences* **120**: e2220570120. https://www.pnas.org/doi/10.1073/pnas.2220570120 (Accessed July 7, 2023).

Fokkens L, Shahi S, Connolly LR, Stam R, Schmidt SM, Smith KM, Freitag M, Rep M. 2018. The multi-speed genome of *Fusarium oxysporum* reveals association of histone modifications with sequence divergence and footprints of past horizontal chromosome transfer events. 465070. https://www.biorxiv.org/content/10.1101/465070v1 (Accessed February 1, 2022).

Fonseca PLC, De-Paula RB, Araújo DS, Tomé LMR, Mendes-Pereira T, Rodrigues WFC, Del-Bem L-E, Aguiar ERGR, Góes-Neto A. 2021. Global characterization of fungal mitogenomes: new insights on genomic diversity and dynamism of coding genes and accessory elements. *Frontiers in Microbiology* **12**. https://www.frontiersin.org/article/10.3389/fmicb.2021.787283 (Accessed April 18, 2022).

Fritsch ES, Chabbert CD, Klaus B, Steinmetz LM. 2014. A genome-wide map of mitochondrial DNA recombination in yeast. *Genetics* **198**: 755–771. https://doi.org/10.1534/genetics.114.166637 (Accessed April 29, 2024).

Garrison E, Guarracino A, Heumos S, Villani F, Bao Z, Tattini L, Hagmann J, Vorbrugg S, Marco-Sola S, Kubica C, et al. 2023. Building pangenome graphs. 2023.04.05.535718. https://www.biorxiv.org/content/10.1101/2023.04.05.535718v1 (Accessed May 3, 2024).

Garrison E, Sirén J, Novak AM, Hickey G, Eizenga JM, Dawson ET, Jones W, Garg S, Markello C, Lin MF, et al. 2018. Variation graph toolkit improves read mapping by representing genetic variation in the reference. *Nat Biotechnol* **36**: 875–879. https://www.nature.com/articles/nbt.4227 (Accessed May 8, 2024).

Guarracino A, Heumos S, Nahnsen S, Prins P, Garrison E. 2022. ODGI: understanding pangenome graphs. *Bioinformatics* **38**: 3319–3326. https://doi.org/10.1093/bioinformatics/btac308 (Accessed May 3, 2024).

Gurdon C, Svab Z, Feng Y, Kumar D, Maliga P. 2016. Cell-to-cell movement of mitochondria in plants. *Proceedings of the National Academy of Sciences* **113**: 3395–3400. https://www.pnas.org/doi/full/10.1073/pnas.1518644113 (Accessed May 17, 2024).

Habig M, Lorrain C, Feurtey A, Komluski J, Stukenbrock EH. 2021. Epigenetic modifications affect the rate of spontaneous mutations in a pathogenic fungus. *Nat Commun* **12**: 5869. https://www.nature.com/articles/s41467-021-26108-y (Accessed April 15, 2023).

Henry PM, Pincot DDA, Jenner BN, Borrero C, Aviles M, Nam M-H, Epstein L, Knapp SJ, Gordon TR. 2021. Horizontal chromosome transfer and independent evolution drive diversification in *Fusarium oxysporum* f. sp. *fragariae*. *New Phytologist* **230**: 327–340. http://onlinelibrary.wiley.com/doi/abs/10.1111/nph.17141 (Accessed September 14, 2022).

Hickey G, Heller D, Monlong J, Sibbesen JA, Sirén J, Eizenga J, Dawson ET, Garrison E, Novak AM, Paten B. 2020. Genotyping structural variants in pangenome graphs using the vg toolkit. *Genome Biol* **21**: 1–17. https://genomebiology.biomedcentral.com/articles/10.1186/s13059-020-1941-7 (Accessed April 26, 2024).

Ingman M, Kaessmann H, Pääbo S, Gyllensten U. 2000. Mitochondrial genome variation and the origin of modern humans. *Nature* **408**: 708–713. https://www.nature.com/articles/35047064 (Accessed April 23, 2024).

Jelen V, de Jonge R, Van de Peer Y, Javornik B, Jakše J. 2016. Complete mitochondrial genome of the Verticillium-wilt causing plant pathogen Verticillium nonalfalfae. *PLoS One* **11**: e0148525. https://www.ncbi.nlm.nih.gov/pmc/articles/PMC4739603/ (Accessed May 24, 2024).

Katoh K, Misawa K, Kuma K, Miyata T. 2002. Mafft: a novel method for rapid multiple sequence alignment based on Fast Fourier transform. *Nucleic Acids Research* **30**: 3059–3066. https://doi.org/10.1093/nar/gkf436 (Accessed April 28, 2023).

Kurian SM, Pietro AD, Read ND. 2018. Live-cell imaging of conidial anastomosis tube fusion during colony initiation in *Fusarium oxysporum* . *PLOS ONE* **13**: e0195634. https://journals.plos.org/plosone/article?id=10.1371/journal.pone.0195634 (Accessed December 22, 2023).

Lang BF, Beck N, Prince S, Sarrasin M, Rioux P, Burger G. 2023. Mitochondrial genome annotation with MFannot: a critical analysis of gene identification and gene model prediction. *Front Plant Sci* **14**. https://www.frontiersin.org/journals/plant-science/articles/10.3389/fpls.2023.1222186/full (Accessed May 3, 2024).

Lang BF, Laforest M-J, Burger G. 2007. Mitochondrial introns: a critical view. *Trends in Genetics* **23**: 119–125. https://www.cell.com/trends/genetics/abstract/S0168-9525(07)00024-8 (Accessed April 16, 2024).

Leducq J-B, Henault M, Charron G, Nielly-Thibault L, Terrat Y, Fiumera HL, Shapiro BJ, Landry CR. 2017. Mitochondrial recombination and introgression during speciation by hybridization. *Molecular Biology and Evolution* **34**: 1947–1959. https://doi.org/10.1093/molbev/msx139 (Accessed April 23, 2024).

Li H, Wang S, Chai S, Yang Z, Zhang Q, Xin H, Xu Y, Lin S, Chen X, Yao Z, et al. 2022. Graph-based pan-genome reveals structural and sequence variations related to agronomic traits and domestication in cucumber. *Nat Commun* **13**: 682. https://www.nature.com/articles/s41467-022-28362-0 (Accessed April 22, 2022).

Li J, Fokkens L, Conneely LJ, Rep M. 2020. Partial pathogenicity chromosomes in Fusarium oxysporum are sufficient to cause disease and can be horizontally transferred. *Environ Microbiol* **22**: 4985–5004.

Li W, Godzik A. 2006. Cd-hit: a fast program for clustering and comparing large sets of protein or nucleotide sequences. *Bioinformatics* **22**: 1658–1659. https://doi.org/10.1093/bioinformatics/btl158 (Accessed May 8, 2024).

Ma L-J, van der Does HC, Borkovich KA, Coleman JJ, Daboussi M-J, Di Pietro A, Dufresne M, Freitag M, Grabherr M, Henrissat B, et al. 2010. Comparative genomics reveals mobile pathogenicity chromosomes in Fusarium. *Nature* **464**: 367–373. https://www.nature.com/articles/nature08850 (Accessed February 3, 2022).

Marçais G, Delcher AL, Phillippy AM, Coston R, Salzberg SL, Zimin A. 2018. MUMmer4: A fast and versatile genome alignment system. *PLOS Computational Biology* **14**: e1005944. https://journals.plos.org/ploscompbiol/article?id=10.1371/journal.pcbi.1005944 (Accessed May 8, 2024).

Maryani N, Lombard L, Poerba YS, Subandiyah S, Crous PW, Kema GHJ. 2019. Phylogeny and genetic diversity of the banana fusarium wilt pathogen *Fusarium oxysporum* f. sp. *cubense* in the Indonesian centre of origin. *Studies in Mycology* **92**: 155–194. https://www.sciencedirect.com/science/article/pii/S0166061618300307 (Accessed May 6, 2022).

McTaggart AR, James TY, Shivas RG, Drenth A, Wingfield BD, Summerell BA, Duong TA. 2021. Population genomics reveals historical and ongoing recombination in the Fusarium oxysporum species complex. *Studies in Mycology* **99**: 100132. https://www.sciencedirect.com/science/article/pii/S0166061621000191 (Accessed August 4, 2023).

Megarioti AH, Kouvelis VN. 2020. The coevolution of fungal mitochondrial introns and their homing endonucleases (GIY-YIG and LAGLIDADG). *Genome Biology and Evolution* **12**: 1337–1354. https://doi.org/10.1093/gbe/evaa126 (Accessed April 18, 2022).

Mehrabi R, Bahkali AH, Abd-Elsalam KA, Moslem M, Ben M'Barek S, Gohari AM, Jashni MK, Stergiopoulos I, Kema GHJ, de Wit PJGM. 2011. Horizontal gene and chromosome transfer in plant pathogenic fungi affecting host range. *FEMS Microbiology Reviews* **35**: 542–554. https://doi.org/10.1111/j.1574-6976.2010.00263.x (Accessed May 23, 2024).

Mehta N, Baghela A. 2021. Quorum sensing-mediated inter-specific conidial anastomosis tube fusion between *Colletotrichum gloeosporioides* and *c. siamense*. *IMA Fungus* **12**: 7. https://doi.org/10.1186/s43008-021-00058-y (Accessed May 22, 2024).

Milani L, Ghiselli F, Guerra D, Breton S, Passamonti M. 2013. A Comparative Analysis of Mitochondrial ORFans: New Clues on Their Origin and Role in Species with Doubly Uniparental Inheritance of Mitochondria. *Genome Biology and Evolution* **5**: 1408–1434. https://doi.org/10.1093/gbe/evt101 (Accessed May 24, 2024).

O'Donnell K, Kistler HC, Cigelnik E, Ploetz RC. 1998. Multiple evolutionary origins of the fungus causing panama disease of banana: concordant evidence from nuclear and mitochondrial gene genealogies. *Proceedings of the National Academy of Sciences* **95**: 2044–2049. http://www.pnas.org/doi/10.1073/pnas.95.5.2044 (Accessed November 25, 2022).

Ondov BD, Treangen TJ, Melsted P, Mallonee AB, Bergman NH, Koren S, Phillippy AM. 2016. Mash: fast genome and metagenome distance estimation using MinHash. *Genome Biology* **17**: 132. https://doi.org/10.1186/s13059-016-0997-x (Accessed June 19, 2024).

Pedregosa F, Varoquaux G, Gramfort A, Michel V, Thirion B, Grisel O, Blondel M, Prettenhofer P, Weiss R, Dubourg V, et al. 2011. Scikit-learn: Machine Learning in Python. *Journal of Machine Learning Research* **12**: 2825–2830. http://jmlr.org/papers/v12/pedregosa11a.html (Accessed June 24, 2022).

Pratt-Hyatt MJ, Kapadia KM, Wilson TE, Engelke DR. 2006. Increased recombination between active tRNA genes. *DNA Cell Biol* **25**: 359–364. https://www.ncbi.nlm.nih.gov/pmc/articles/PMC3756803/ (Accessed May 23, 2024).

Price MN, Dehal PS, Arkin AP. 2010. FastTree 2 – Approximately maximum-likelihood trees for large alignments. *PLOS ONE* **5**: e9490. https://journals.plos.org/plosone/article?id=10.1371/journal.pone.0009490 (Accessed May 13, 2024).

Quevillon E, Silventoinen V, Pillai S, Harte N, Mulder N, Apweiler R, Lopez R. 2005. InterProScan: protein domains identifier. *Nucleic Acids Res* **33**: W116–W120. https://www.ncbi.nlm.nih.gov/pmc/articles/PMC1160203/ (Accessed May 8, 2024).

Quinlan AR, Hall IM. 2010. BEDTools: a flexible suite of utilities for comparing genomic features. *Bioinformatics* **26**: 841–842.

Read ND, Goryachev AB, Lichius A. 2012. The mechanistic basis of self-fusion between conidial anastomosis tubes during fungal colony initiation. *Fungal Biology Reviews* **26**: 1–11. https://www.sciencedirect.com/science/article/pii/S174946131200005X (Accessed May 22, 2024).

Repar J, Warnecke T. 2017. Mobile introns shape the genetic diversity of their host genes. *Genetics* **205**: 1641–1648. https://www.ncbi.nlm.nih.gov/pmc/articles/PMC5378118/ (Accessed April 25, 2024).

Rice DW, Alverson AJ, Richardson AO, Young GJ, Sanchez-Puerta MV, Munzinger J, Barry K, Boore JL, Zhang Y, dePamphilis CW, et al. 2013. Horizontal transfer of entire genomes via mitochondrial fusion in the angiosperm amborella. *Science* **342**: 1468–1473. https://www.science.org/doi/10.1126/science.1246275 (Accessed May 14, 2024).

Roca MG, Davide LC, Mendes-Costa MC, Wheals A. 2003. Conidial anastomosis tubes in *Colletotrichum*. *Fungal Genetics and Biology* **40**: 138–145. https://www.sciencedirect.com/science/article/pii/S1087184503000884 (Accessed May 14, 2024).

Sellem CH, Belcour L. 1997. Intron open reading frames as mobile elements and evolution of a group I intron. *Mol Biol Evol* **14**: 518–526.

Shahi S, Beerens B, Bosch M, Linmans J, Rep M. 2016. Nuclear dynamics and genetic rearrangement in heterokaryotic colonies of *Fusarium oxysporum*. *Fungal Genet Biol* **91**: 20–31.

Sherman RM, Salzberg SL. 2020. Pan-genomics in the human genome era. *Nat Rev Genet* **21**: 243–254. https://www.nature.com/articles/s41576-020-0210-7 (Accessed January 10, 2023).

Shimoyama Y. 2022. pyGenomeViz: A genome visualization python package for comparative genomics. https://github.com/moshi4/pyGenomeViz.

Sirén J, Monlong J, Chang X, Novak AM, Eizenga JM, Markello C, Sibbesen JA, Hickey G, Chang P-C, Carroll A, et al. 2021. Pangenomics enables genotyping of known structural variants in 5202 diverse genomes. *Science* **374**: abg8871. https://www.science.org/doi/10.1126/science.abg8871 (Accessed May 8, 2024).

Smith DR, Keeling PJ. 2015. Mitochondrial and plastid genome architecture: Reoccurring themes, but significant differences at the extremes. *Proceedings of the National Academy of Sciences* **112**: 10177–10184. https://www.pnas.org/doi/full/10.1073/pnas.1422049112 (Accessed April 23, 2024).

Spinelli JB, Haigis MC. 2018. The multifaceted contributions of mitochondria to cellular metabolism. *Nat Cell Biol* **20**: 745–754. https://www.nature.com/articles/s41556-018-0124-1 (Accessed April 23, 2024).

Stamatakis A. 2014. RAxML version 8: a tool for phylogenetic analysis and post-analysis of large phylogenies. *Bioinformatics* **30**: 1312–1313. https://doi.org/10.1093/bioinformatics/btu033 (Accessed October 20, 2023).

van Dam P, Fokkens L, Ayukawa Y, van der Gragt M, ter Horst A, Brankovics B, Houterman PM, Arie T, Rep M. 2017. A mobile pathogenicity chromosome in *Fusarium oxysporum* for infection of multiple cucurbit species. *Sci Rep* **7**: 9042. https://www.nature.com/articles/s41598-017-07995-y (Accessed February 3, 2022).

van Westerhoven AC, Aguilera-Galvez C, Nakasato-Tagami G, Shi-Kunne X, Martinez de la Parte E, Chavarro-Carrero E, Meijer HJG, Feurtey A, Maryani N, Ordóñez N, et al. 2024. Segmental duplications drive the evolution of accessory regions in a major crop pathogen. *New Phytologist* **242**: 610–625. https://onlinelibrary.wiley.com/doi/abs/10.1111/nph.19604 (Accessed May 13, 2024).

Vangalis V, Knop M, Typas MA, Papaioannou IA. 2021. Establishment of conidial fusion in the asexual fungus Verticillium dahliae as a useful system for the study of non-sexual genetic interactions. *Curr Genet* **67**: 471–485. https://doi.org/10.1007/s00294-021-01157-4 (Accessed May 14, 2024).

Vlaardingerbroek I, Beerens B, Schmidt SM, Cornelissen BJC, Rep M. 2016. Dispensable chromosomes in *Fusarium oxysporum* f. sp. *lycopersici*. *Molecular Plant Pathology* **17**: 1455–1466. https://onlinelibrary.wiley.com/doi/abs/10.1111/mpp.12440 (Accessed February 3, 2022).

Wang B, Liang X, Hao X, Dang H, Hsiang T, Gleason ML, Zhang R, Sun G. 2021. Comparison of mitochondrial genomes provides insights into intron dynamics and evolution in Botryosphaeria dothidea and B. kuwatsukai. *Environmental Microbiology* **23**: 5320–5333. http://onlinelibrary.wiley.com/doi/abs/10.1111/1462-2920.15608 (Accessed November 23, 2022).

Wang N, Li C, Kuang L, Wu X, Xie K, Zhu A, Xu Q, Larkin RM, Zhou Y, Deng X, et al. 2022a. Pan-mitogenomics reveals the genetic basis of cytonuclear conflicts in citrus hybridization, domestication, and diversification. *Proceedings of the National Academy of Sciences* **119**: e2206076119. https://www.pnas.org/doi/abs/10.1073/pnas.2206076119 (Accessed February 10, 2023).

Wang T, Antonacci-Fulton L, Howe K, Lawson HA, Lucas JK, Phillippy AM, Popejoy AB, Asri M, Carson C, Chaisson MJP, et al. 2022b. The Human Pangenome Project: a global resource to map genomic diversity. *Nature* **604**: 437–446. https://www.nature.com/articles/s41586-022-04601-8 (Accessed April 26, 2024).

Wick RR, Schultz MB, Zobel J, Holt KE. 2015. Bandage: interactive visualization of de novo genome assemblies. *Bioinformatics* **31**: 3350–3352. https://doi.org/10.1093/bioinformatics/btv383 (Accessed May 3, 2024).

Wu B, Buljic A, Hao W. 2015. Extensive horizontal transfer and homologous recombination generate highly chimeric mitochondrial genomes in yeast. *Molecular Biology and Evolution* **32**: 2559–2570. https://doi.org/10.1093/molbev/msv127 (Accessed April 11, 2024).